

Electronic structure of the GaAs(114)A-(2×1) and GaAs(114)B-(2×1) surfaces

R. D. Smardon and G. P. Srivastava

School of Physics, University of Exeter, Stocker Road, Exeter, EX4 4QL, United Kingdom

(Received 1 December 2004; revised manuscript received 28 March 2005; published 8 July 2005)

Ab initio density functional theory calculations, based on pseudopotentials and the plane wave formalism, have been pursued to examine the equilibrium geometry, bonding and electronic structure of the previously studied GaAs(114)A- $\alpha 2(2 \times 1)$ surface and in addition a newly proposed GaAs(114)B- $\alpha 2(2 \times 1)$ surface. Both stoichiometric surfaces are characterized by three prominent surface features (dimers, tetramers, and rebonded atoms). Several surface states are found in and around the bulk band gap and are interpreted by simulated STM images as well as k -point analysis.

DOI: 10.1103/PhysRevB.72.035317

PACS number(s): 68.47.Fg, 71.15.Mb, 71.15.Pd, 71.20.Nr

I. INTRODUCTION

High index semiconductor surfaces are technologically important and fundamentally interesting to study. Such high index surfaces show the potential of supporting overlayer growth of quantum wires¹ and quantum dots,² which are useful in device applications. Even the growth of quantum dot structures on host low index surfaces have displayed the existence of high index facets leading to the proposal that high index surfaces may indeed be atomically flat and stable.³ Indeed the existence of stable GaAs(113), GaAs(114), and GaAs(2 5 11) surfaces have been observed from molecular beam epitaxy (MBE) grown samples.⁴ Generally to support the growth of atomic size devices the substrate surface is required to be flat, with a low surface energy. It has been previously reported that GaAs(114) indeed fulfills these requirements.⁵ However, if any real progress is to be made in device growth optimization, not only is a detailed atomic geometry required, but also the electronic properties associated with these surfaces.

The morphology of high index surfaces is intimately correlated with the angle of orientation away from the densely-packed lower index planes. For nonpolar high index surfaces such as Si(114), large angular offsets produce grooved, sawtooth-like surfaces, whereas small angles lead to vicinal surfaces made up of (001) terraces separated by occasional steps.⁶ For surfaces with an orientation greater than 5° away from the low index (001) surface, as is the case with (114) surfaces, a large proportion of the resulting (001) terraces possess dimers orientated parallel to the step edges (*B*-type terraces). Between the primary growth and cleavage planes of Si [i.e., the (100) and (111) planes respectively], numerous different surfaces may be formed, with varying degrees of stability.⁷ The existence of plausible stable high index surfaces between (001) and (111) planes for polar semiconductors, e.g., GaAs(114), cannot be easily inferred from the above understanding of high index silicon surfaces. This is primarily due to two possible terminations (cationic and anionic) for polar surfaces. The (110) natural cleavage plane is nonpolar, but does not lie between the (001) and the (111) surfaces.

The GaAs(114) surface is inclined 19.5° from the (001) plane in the direction of the (111) plane and comprises (001)-type terraces separated by double layer (DL) steps.⁷ For both

nonpolar as well as polar semiconductors, surface geometry from the (001) to (117) planes can generally be described in terms of (001)-type terraces separated by double layer steps. The stress and dangling bond density of surfaces between (001) to (117) planes is reduced by the formation of rebonded atoms at step edges. A schematic representation of the (114) and (117) planes along these lines is given in Fig. 1. The surface energy can be further reduced by the inclusion of nonrebonded atoms also at the step edges on the surfaces between (117) and (114) inclusive. It is this combination of rebonded and nonrebonded atoms at step edges that leads to a highly stable surface geometry for both polar and nonpolar semiconductor surfaces.^{8,9} The GaAs(114) surface exhibits what has been termed an $\alpha 2(2 \times 1)$ reconstruction, whose structure has been proposed and verified with STM imaging by Márquez *et al.*⁸ Further work by Márquez *et al.*¹¹ has provided theoretically determined relaxed atomic geometries of the $\alpha 2(2 \times 4)$ and $\beta 2(2 \times 4)$ reconstructions of GaAs(114)A.

As illustrated in Fig. 2, the basic constituents of this surface reconstruction are dimer formation and same-species rebonding. Along $[\bar{1}10]$ a *B*-type dimer is formed by the atoms labeled *A*. Atoms *C* form another *B*-type dimer in the same direction (termed tetramer bridge). A tetramer is formed between atoms *C* and *D* and the bonds between atoms *C* and *D* could be considered as *A*-type dimers (termed tetramer

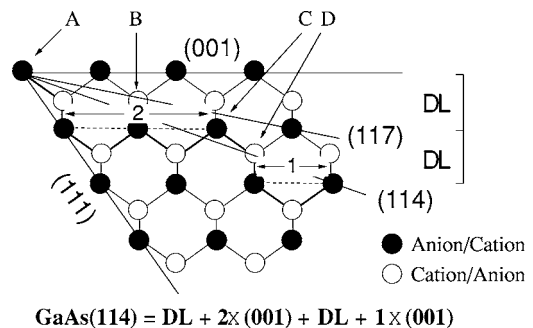


FIG. 1. A schematic representation of a few planes from (001) through to (111) for a tetrahedrally bonded crystalline material. Single and double width (001) terraces are indicated by the numbers 1 and 2, respectively. DL represents a double layer step. Other symbols are explained in the text.

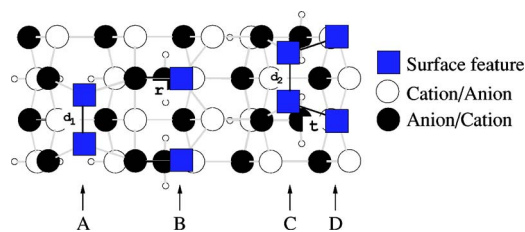


FIG. 2. (Color online) A schematic representation of a top view of the supercell used in our calculations modeling the GaAs(114)- $\alpha 2(2 \times 1)$ surfaces. d_1 and d_2 represent dimers formed along the $[\bar{1}10]$ direction, r and t label rebonded and nonrebonded step edge bonds.

arms). The formation of dimers is in close analogy with the (2×1) reconstruction of nonpolar (001) surfaces, whereby the A-type (B-type) dimers are perpendicular (parallel) to the step edge. The formation of dimers lowers the surface energy by decreasing the number of unsaturated dangling bonds. The atoms labeled B are rebonded atoms. The surface energy is further decreased when these atoms saturate some of their dangling bonds and increase their coordination number. This rebonding occurs at the step edge, following the proposal made by Chadi.¹⁰ The surface unit cell thus exhibits a series of DL, B-type (001) terraces separated by rebonded and nonrebonded steps. This is schematically illustrated in Fig. 1.

The GaAs(114) surface is stoichiometric, i.e., within the surface layer there are an equal number of cationic and anionic species. This leads to two plausible stable surface reconstructions: the previously reported GaAs(114)A- $\alpha 2(2 \times 1)$ structure^{8,11} and, following the labeling convention, a new GaAs(114)B- $\alpha 2(2 \times 1)$ surface. The terminology for the (114)A and (114)B surfaces is rather similar to that used for the (111)A and (111)B surfaces. The (111)A/(111)B surface is terminated at the cationic or anionic atomic layer. Consistent with this terminology we will refer to the (114)A/(114)B surface if it is characterized with cation or anion step-mediating atoms [i.e., rebonded (B) and nonrebonded (D) atoms] as well as anion-anion or cation-cation dimer (A and C) atoms, as schematically illustrated in Fig. 2.

To the best of our knowledge, there are no previously published results for the GaAs(114)B- $\alpha 2(2 \times 1)$ surface or for the detailed electronic structure (i.e., E versus k dispersion curves) of either GaAs(114)A- $\alpha 2(2 \times 1)$ or GaAs(114)B- $\alpha 2(2 \times 1)$ surfaces. This work presents a study of the surface geometry, electronic structure, and simulated STM images for these surfaces. In addition, the bonding nature of the surface orbitals are provided and discussed. We compare our atomic geometry with that of Márquez *et al.*^{8,11} for the A surface and provide a more detailed discussion of simulated STM images of both the A and B surfaces at various positive and negative biases.

II. METHODOLOGY

The results of all calculations presented in this paper are based on density functional theory within the local density approximation. The parametrized Perdew and Zunger¹² form

of the Ceperley-Alder¹³ electron correlation scheme was used, and electron-ion interactions were described by the norm-conserving pseudopotentials of Troullier and Martins.¹⁴ The relaxation of atomic and electronic degrees of freedom was achieved by solving the dynamic Kohn-Sham equations by a Car-Parrinello-like approach within a plane wave basis set.^{15,16}

The surface was modeled in a periodic slab geometry, the unit cells having the natural periodicity of the surface and an invoked artificial periodicity normal to the surface. Twelve layers of bulk GaAs with an equivalent 12 layers of vacuum were modeled. The “active” surface was investigated while the opposite face of the slab was passivated with fractionally charged hydrogen ($1.25e$ and $0.75e$ for Ga and As dangling bonds, respectively). One layer of atoms, adjacent to the passivating (hydrogen) atoms, was kept frozen in the bulk position and all other atoms were allowed to relax into their minimum energy configuration. The surface geometry and electronic structure was obtained using a 12 Ryd kinetic energy cut-off. Test runs at 8, 10, 12, and 14 Ryd cutoffs revealed that the structural and electronic parameters were well converged at the 12 Ryd value. The theoretical bulk lattice constant of 5.62 \AA was used in the surface calculations. Four special k points were used throughout for the sampling of the irreducible part of the Brillouin zone.¹⁷

III. RESULTS

A. Atomic structure

The structural relaxation of the GaAs(114)- (2×1) surfaces are characterized by three main features, as shown in Fig. 2. These are: a dimer (A); rebonded atoms (B); and a tetramer (C and D). Both the GaAs(114)A- $\alpha 2(2 \times 1)$ and GaAs(114)B- $\alpha 2(2 \times 1)$ surfaces display these three features, although with different orientations according to the surface termination. These three surface components characterize the (114) surfaces of zinc blende as well as diamond-structure semiconductors.^{7,9,18} The feature A on the GaAs(114) surfaces is similar to those present on the GaAs(001) surfaces. The same-species rebonded atoms (B) arise from one of the two inequivalent DL step edges within the unit cell. Upon reconstruction each rebonded atom saturates one of its two dangling bonds with an adjacent dangling bond over a step edge. The relaxation of each of these three features on GaAs(114) is expected to show some differences from the corresponding features on Si(114). First, while the tilt of the A dimer on Si(114) results from charge transfer from one component to the other, there is no asymmetric tilting of this feature on GaAs(114) as the dangling bond on both dimer components are either fully saturated or fully empty. Secondly, a tetramer arm being comprised of two different atomic species on GaAs(114) is likely to experience a charge transfer from the cation to the anion analogous to the physics of the III-V(110) surfaces. Thus the relative heights of the C and D components of the tetramer are expected to be different depending on the orientation of the GaAs(114) surface. Consistent with the above stated relaxation mechanisms, and contrary to the Si(114)- (2×1) surface,⁹ upon relaxation,

TABLE I. The average displacements of the features *A*, *B*, *C*, and *D* from their ideal bulk positions along the directions indicated in Figs. 3 and 4, expressed in angstroms. The values given in parenthesis are those calculated in Ref. 11. For the dimer features *A* and *C* the value shown ($|\Delta[\bar{1}10]|$) is the displacement from the bulk towards its bonding partner.

	$\Delta[\bar{2}21]$	$ \Delta[\bar{1}10] $	$\Delta[114]$
GaAs(114)A- $\alpha 2(2 \times 1)$			
Dimer-A	0.25 (0.23)	0.73 (0.72)	0.28 (0.26)
Rebonded atom-B	1.10 (1.19)	0.00 (0.03)	-0.72 (-0.73)
Tetramer dimer-C	0.13 (0.15)	0.74 (0.73)	0.17 (0.19)
Nonrebonded atom-D	0.47 (0.50)	0.12 (0.13)	-0.37 (-0.33)
GaAs(114)B- $\alpha 2(2 \times 1)$			
Dimer-A	0.54	0.72	-0.31
Rebonded atom-B	0.93	0.00	-0.10
Tetramer dimer-C	0.21	0.75	-0.49
Nonrebonded atom-D	0.11	0.00	0.30

only one distinct local structural minimum was located for the GaAs(114)A- $\alpha 2(2 \times 1)$ and GaAs(114)B- $\alpha 2(2 \times 1)$ surfaces.

The theoretical investigation by Márquez *et al.* has concluded that the GaAs(114)A- $\alpha 2(2 \times 1)$ surface has a stable configuration. From our total energy calculations both surfaces were found to be of similar energy. Only a small energy difference was found between them, of 3 meV/Å² in favor of the GaAs(114)A surface. This suggests the both the *A* and *B* surfaces are equally stable. Thus a detailed investigation of the atomic geometries of both surfaces would be appropriate. Our calculated structural parameters have been interpreted in Table I for both *A* and *B* surfaces with respect to the ideal bulk configuration. This also allows a direct comparison between the results obtained for the *A* surface by Márquez *et al.*¹¹ and the results presented here. The information in Table I can also be of use to compare with any future experimental analysis of x ray standing wave studies. It can be seen that in general our results for the *A* surface are in very good agreement with those of Márquez *et al.* Specifically both results agree excellently on the displacement of dimer components from their bulk positions, each of which contracts by 18% towards the other. This result agrees with the well observed phenomenon of dimer formation on the (100) surface of polar and nonpolar semiconductors. The *B* surface shows atomic displacements similar to the *A* surface, but with different magnitudes due to different chemical species involved.

The results presented in Table II have been interpreted from Table I in a more physically appealing form characterizing the relaxed surfaces as shown in Figs. 3 and 4. For the (114)A surface, the As dimer lengths d_1 and d_2 are found to be very similar, approximately 2.50 Å. This length is also very close to the As dimer length on the GaAs(001) surface.¹⁹ For the (114)B surface, the Ga dimer lengths d_1 and d_2 are also very similar, approximately 2.47 Å. This dimer length is, again, very similar to the Ga dimer length on

TABLE II. Calculated values of the key structural parameters shown in Figs. 3 and 4 for the GaAs(114)A- $\alpha 2(2 \times 1)$ and GaAs(114)B- $\alpha 2(2 \times 1)$ surfaces. Δ_D , Δ_{TD} , Δ_{NR} , and Δ_R are the vertical heights (above subsurface atom S) for the dimer, tetramer-dimer, nonrebonded, and rebonded atoms, respectively. The angles displayed are the $[2\bar{2}1]$ plane projected angles in degrees and the bond lengths are in Å.

Structural parameter	GaAs(114)A- $\alpha 2(2 \times 1)$	GaAs(114)B- $\alpha 2(2 \times 1)$
Δ_D	1.42	0.81
$\angle D$	96.0	133.8
d_1	2.50	2.48
Δ_{TD}	1.99	1.30
$\angle TD$	91.4	147.4
d_2	2.49	2.46
Δ_{NR}	0.79	1.43
$\angle NR$	172.4	95.0
<i>t</i>	2.33	2.25
Δ_R	1.09	1.69
$\angle R$	147.8	102.4
<i>r</i>	2.57	2.54

the GaAs(001) surface.²⁰ These results suggest that surface dimer lengths tend to be conserved quantities, supporting a previous hypothesis.²¹ The maximum difference for a given dimer bond length on the (114) and the (001) surfaces is 1%. The near equality of dimer lengths on the (001) and (114) surfaces suggests that there is a mechanism for stress relief on the (114) surface along the direction perpendicular to the dimer line. The surface Ga atoms lie closer to their substrate neighbors in accordance with their desire to form a planar *sp*² bonding configuration. This is clearly seen in Table II where angles $\angle R$ and $\angle NR$ on the *A* surface, and angles $\angle D$ and $\angle TD$ on the *B* surface, are much larger than the tetrahedral angle. On the other hand, the surface As atoms lie far-

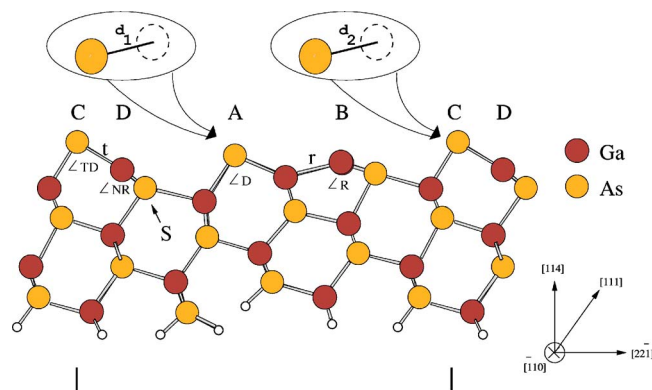


FIG. 3. (Color online) A schematic representation of the side profile of the GaAs(114)A- $\alpha 2(2 \times 1)$ surface used in our calculations. *A*: dimer atoms; *B*: rebonded atoms; and *C* and *D* form a tetramer (*C*: dimer atoms; *D*: nonrebonded step atoms). Other symbols are explained within the text.

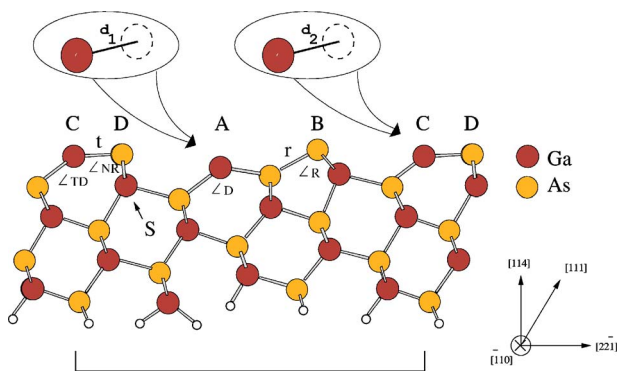


FIG. 4. (Color online) A schematic representation of the side profile of the GaAs(114)B- $\alpha 2(2 \times 1)$ surface. The labeling convention is taken from Fig. 3 and is also explained in the text.

ther from their substrate neighbors with their desire to form a pyramidal s^2p^3 bonding configuration. This is clearly seen Table II where angles $\angle D$ and $\angle TD$ on the A surface, and angles $\angle R$ and $\angle NR$ on the B surface, are much smaller than the tetrahedral angle.

The bonds r , formed by the rebonded atoms, undergo a 5% and 1% increase for the GaAs(114)A and GaAs(114)B surfaces, respectively, when compared to the same-species dimer length. These extended bonds are caused by the strained nature of the rebonding near the step edge. The larger increase in bond length for the Ga-Ga bond on the GaAs(114)A surface originates from the withdrawal of some charge by the adjacent As dimer. The As-As bond on the GaAs(114)B surface conserves its length (within 1%) by attracting charge from the neighboring Ga dimer.

The other step mediating bonds t are formed between each dimerlike tetramer atoms C and its adjacent nonrebonded tetramer atoms D. For both A and B surfaces these are always mixed species (Ga and As). Being perpendicular to the step edge, these tetramer arms are some 6% and 9% shorter when compared to the same species bond lengths stated above for the A and B surfaces, respectively. These heterodimer Ga-As bond lengths on the (114) surfaces are also shorter than the mixed-species surface back-bond length on the gallium-rich GaAs(001) surface,²⁰ which in turn are both shorter than the bulk Ga-As bulk bond length. This bond constriction may be explained to arise from the electrostatic force driving the more electronegative As atom away from the bulk. The percentage decrease in the tetramer arm length t is similar to the shortening of the surface bond length on III-N(110) surfaces, but more significant than on the (110) surface of non-nitride semiconductors (see, e.g., Ref. 22). The longer and shorter r and t bonds perpendicular to the B-type dimer line on the (114) surface provide a clearer signature of a stress relief mechanism. Consistent with the electrostatic arguments presented above, Table II also shows that the angle subtended at the surface Ga atom is larger than the angle at the surface As atoms.

B. Electronic structure

The electronic structures, obtained within the LDA, are shown in Figs. 5 and 6 for the GaAs(114)A and GaAs(114)B

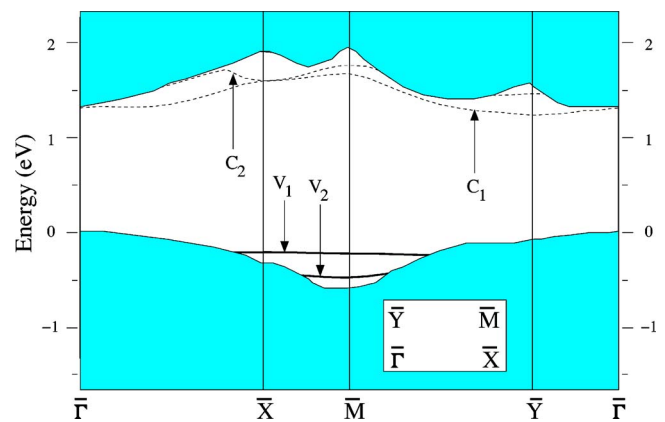


FIG. 5. (Color online) Calculated band structure for the GaAs(114)A- $\alpha 2(2 \times 1)$ surface. The surface bands are shown as heavy solid (occupied) and dashed (unoccupied) lines against the (2×1) -projected bulk structure for GaAs(114). The energy zero is set at the bulk valence band edge.

surfaces, respectively. It is well known that the application of the LDA results in an underestimation of the band gap in a semiconductor. However, a quasiparticle calculation (not presented here) is expected to result in a similar level of band gap opening for both the GaAs(114)A and GaAs(114)B surfaces. In this section we will discuss the LDA results. Our calculations suggest that the electronic structure of both surfaces exhibits a rich spectrum of surface bands within and around the GaAs bulk band gap. Generally, these localized surface electronic bands display relatively little dispersion.

For the GaAs(114)A- $\alpha 2(2 \times 1)$ surface there are two occupied surface bands (both lie below the bulk valence band edge) and two unoccupied surface bands (one lying partly below the bulk conduction band edge and the other wholly above). The band gap between the highest occupied surface state V_1 at \bar{X} and the lowest unoccupied surface state C_1 at \bar{Y} is approximately 1.4 eV. The highest occupied state (V_1) is derived from the p_z orbitals localized at atoms on both As dimers on the top surface layer (i.e., at atoms A and C in Fig.

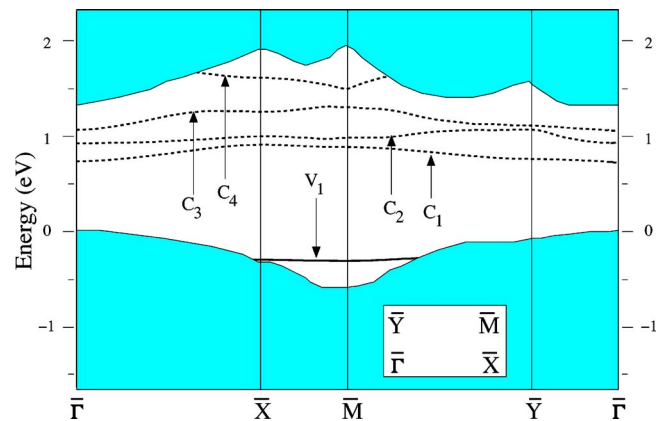


FIG. 6. (Color online) Calculated band structure for the GaAs(114)B- $\alpha 2(2 \times 1)$ surface. The surface bands are shown as heavy solid (occupied) and dashed (unoccupied) lines against the (2×1) -projected bulk structure for GaAs(114). The energy zero is set at the bulk valence band edge.

3). The second highest occupied surface state V_2 is only localized around the \bar{M} -point and also originates from the p_z orbitals on the two As dimers. The lowest unoccupied state (C_1) is always predominantly localized on the rebonding atom with a small contribution from the tetramer. The orbital nature of this state at the rebonded atom is p_z , while the smaller contribution from the tetramer is sp^2 in nature and is found to exist within the plane formed by the tetramer dimer and the nonrebonded step edge atoms (i.e., the plane containing atoms C and D in Fig. 3). The band C_2 shows the same properties as exhibited by C_1 .

With one occupied surface band (lying below the bulk valence band edge) and four unoccupied surface bands (3 lying partly wholly below the bulk conduction band edge and one other wholly above), the GaAs(114)B- $\alpha 2(2 \times 1)$ surface also presents a dense array of surface localized bands within the GaAs bulk band gap. An energy separation of 1.0 eV divides an indirect band gap between the highest occupied state at \bar{X} and the lowest unoccupied state at $\bar{\Gamma}$. The band V_1 at \bar{X} and \bar{M} is characterized by p_z orbitals of the surface-plane As species (see Fig. 4, atoms B and D). This electronic feature reconfirms the structural result presented earlier in that although the bulk termination of the GaAs(114)B surface has the Ga species of the tetramer dimer as its highest lying surface atoms, upon relaxation it is the more electronegative As species (atoms B and D) that become the highest-lying on the surface. The unoccupied bands C_1 , C_2 , and C_3 are located wholly below the conduction band edge and show comparatively little dispersion along the symmetry directions. C_4 also manifests itself as a flat band, but it lies totally above the conduction band edge. The bands C_1 , C_2 , and C_3 are a resultant of the electron depleted Ga dimer orbitals (depleted due to the electrostatic drawing of charge to neighboring As atoms) and empty states localized on the rebonding atoms B in Fig. 4. The band C_4 is localized primarily upon both the Ga dimers with a significantly less rebonding contribution.

We have simulated constant-current STM images, within the Tersoff-Hamann formalism,²³ which computes contours of constant local density of states in the surface region within a voltage bias with respect to the Fermi energy. Details of our numerical scheme can be found in Miotto *et al.*²⁴ The results for the occupied and the unoccupied states for the GaAs(114)A- $\alpha 2(2 \times 1)$ and GaAs(114)B- $\alpha 2(2 \times 1)$ surfaces have been presented in Figs. 7, 8, and 9. In order to facilitate a clear discussion of the voltage dependence of the STM images we have presented several simulations at various biases.

The occupied-state images for the GaAs(114)A surface have been calculated at biases -2.5 , -2.0 , and -1.5 eV relative to the Fermi level. It can be seen that with decreasing bias towards the Fermi level the brightness of both dimers, i.e., the dimer associated with the tetramer and the nonstep edge dimer, becomes less pronounced. This effect is also seen for the rebonding atoms and the rebonding back-bond atoms (the mediating atoms between the tetramer and the rebonding atoms). Our images bear some agreement, and yet there are some discrepancies, with the experimental and simulated STM images (for a bias of -2.5 eV) obtained by

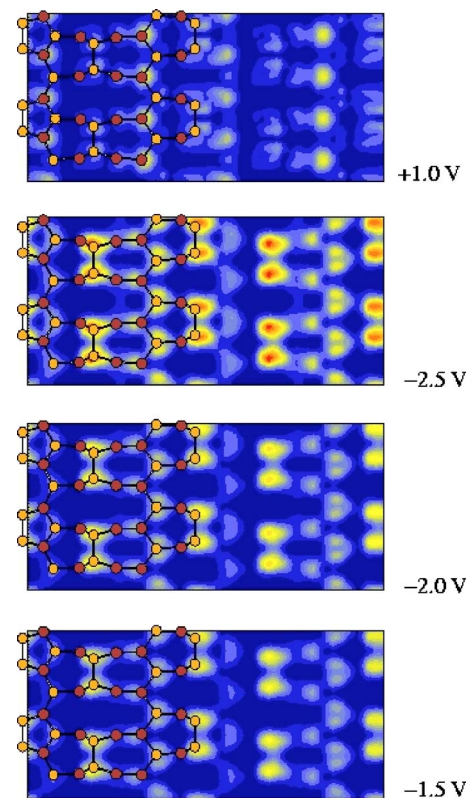


FIG. 7. (Color online) Simulated occupied and unoccupied state images of the GaAs(114)A- $\alpha 2(2 \times 1)$ surface. The occupied states are reported with biases of -2.5 , -2.0 , and -1.5 eV relative to the Fermi level. The unoccupied image corresponds to a bias of $+1.0$ eV.

Márquez *et al.*¹¹ The STM images in the work by Márquez *et al.* shows a large contribution from just the As dimer atoms in the tetramer, with a smaller yield from the other surface features. In contrast, our results indicate an almost equal brightness for both the dimers, consistent with detailed \bar{k} -point analysis of the bands V_1 and V_2 discussed above. The almost equal contribution from the two inequivalent placed surface dimers within the unit cell is not surprising. The dangling bonds of the two dimers are fully occupied and have given rise to two closely positioned states V_1 and V_2 . A similar situation has also been observed for the energy states originating from the 1st and 3rd layer As dimers on the GaAs(001)- $\beta 2(2 \times 4)$ surface.¹⁹ The simulated STM image for the unoccupied states for the GaAs(114)A- $\alpha 2(2 \times 1)$ surface is also presented in Fig. 7 at a bias of $+1.0$ eV. It consists mainly of states associated with the dangling bonds at the Ga rebonding atoms with a small contribution from the Ga atoms of the tetramer. The observations for the occupied and un-occupied states to correspond to the surface As and Ga atoms, respectively, are consistent with the electron counting rule, whereby As draws more electrical charge towards itself, whilst Ga prefers to donate charge.

The simulated STM images for the GaAs(114)B- $\alpha 2(2 \times 1)$ surface is provided in Figs. 8 and 9. The occupied surface states for GaAs(114)B- $\alpha 2(2 \times 1)$ shown in Fig. 8 has been calculated for a few biases (-2.5 , -2.0 , -1.5 , and -1.0 eV) relative to the Fermi level. The images exhibit

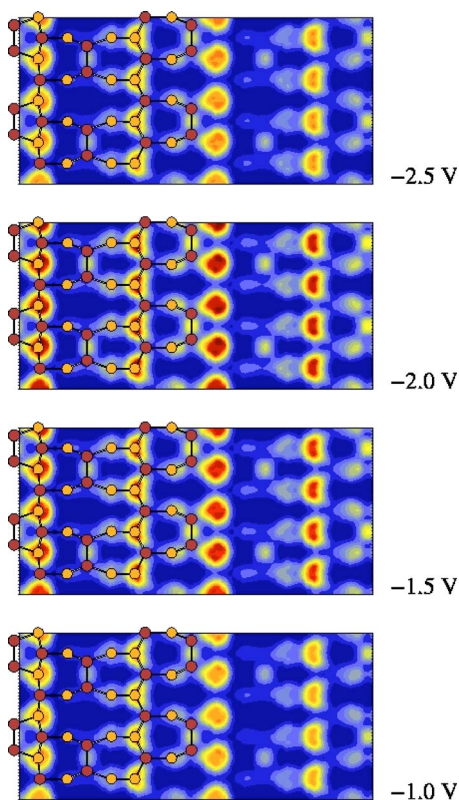


FIG. 8. (Color online) Simulated occupied state images of the GaAs(114) B - $\alpha 2(2 \times 1)$ surface. The occupied states are reported with biases of -2.5 , -2.0 , -1.5 , and -1.0 eV relative to the Fermi level.

strong features related to the As species upon the surface belonging to the rebonding atoms and the tetramer: these features are most intense between the biases of -2.0 and -1.5 eV. The unoccupied surface states for this surface are exhibited in Fig. 9 and show mainly Ga connected features from the empty dangling bonds of the dimer features A and C , at various biases ($+0.5$, $+1.0$, and $+1.5$ eV). However, there is a small contribution from the As rebonding atoms (feature B) up to $+1.0$ eV from the Fermi level, but this begins to decrease with increasing bias. This indicates that compared to the rebonding features, the dimer features produce a relatively large number of states with more of these contributing with increase in bias sampling.

IV. CONCLUSION

In conclusion, this paper has presented results of *ab initio* calculations of the geometry, electronic structure and simu-

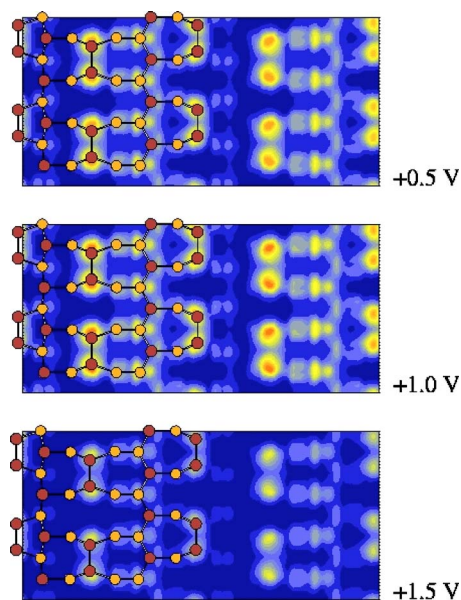


FIG. 9. (Color online) Simulated unoccupied state images of the GaAs(114) B - $\alpha 2(2 \times 1)$ surface. The unoccupied images correspond to biases of $+0.5$, $+1.0$, and $+1.5$ eV relative to the Fermi level.

lated STM images of the reconstructed GaAs(114) A - $\alpha 2(2 \times 1)$ and GaAs(114) B - $\alpha 2(2 \times 1)$ surfaces. These high index surfaces appear to reconstruct in a manner to support the electrostatic favoring of higher lying surface As atoms with approximately $3 \text{ meV}/\text{\AA}^2$ between the two surfaces in favor of the GaAs(114) A - $\alpha 2(2 \times 1)$ surface. Our structural features for the A surface are in good agreement with those presented by Márquez *et al.*, thus justifying the results presented here for the newly proposed B surface. Both surfaces are characterized by a number of localized states in and around the bulk band gap region. The surface band gap is 1.4 eV and 1.0 eV for the GaAs(114) A and GaAs(114) B surfaces, respectively. The characteristics these surface states have been explained by examining simulated STM images and k -point analysis. It is concluded that for both of the GaAs(114) A - $\alpha 2(2 \times 1)$ and GaAs(114) B - $\alpha 2(2 \times 1)$ surfaces it is mainly the As species that give rise to the occupied surface states, whereas it is the Ga atoms that are responsible for the unoccupied states. An experimental investigation of the electronic states on the GaAs(114) B - $\alpha 2(2 \times 1)$ surface would be desirable.

ACKNOWLEDGMENT

R.D.S. gratefully acknowledges financial support from the EPSRC(UK).

¹R. Nötzel, J. Menniger, M. Ramsteiner, A. Ruiz, H.-P. Schönherr, and K. H. Ploog, Appl. Phys. Lett. **68**, 1132 (1996); A. Richter, G. Behme, M. Stüptitz, C. Lienau, T. Elsaesser, M. Ramsteiner, R. Nötzel, and K. H. Ploog, Phys. Rev. Lett. **79**, 2145 (1997).
²R. Nötzel, Z. Niu, M. Ramsteiner, H.-P. Schönherr, A. Tampert, L. Däweritz, and K. H. Ploog, Nature (London) **392**, 56 (1998).

³Y. Hasegawa, H. Kiyama, Q. K. Xue, and T. Sakurai, Appl. Phys. Lett. **72**, 2265 (1998).

⁴L. Geelhaar, Y. Temko, J. Márquez, P. Kratzer, and K. Jacobi, Phys. Rev. B **65**, 155308 (2002); K. Jacobi, L. Geelhaar, and J. Márquez, Appl. Phys. A: Mater. Sci. Process. **75**, 113 (2002).

⁵K. Jacobi, L. Geelhaar, J. Márquez, J. Platen, and C. Setzer, Appl.

- Surf. Sci. **166**, 173 (2000).
- ⁶B. S. Swartzentruber, N. Kitamura, M. G. Lagally, and M. B. Webb, Phys. Rev. B **47**, 13432 (1993).
- ⁷A. A. Baski, S. C. Erwin, and L. J. Whitman, Surf. Sci. **392**, 69 (1997).
- ⁸J. Márquez, P. Kratzer, L. Geelhaar, K. Jacobi, and M. Scheffler, Phys. Rev. Lett. **86**, 115 (2001).
- ⁹R. D. Smardon, G. P. Srivastava, and S. J. Jenkins, Phys. Rev. B **69**, 085303 (2004).
- ¹⁰J. Márquez, P. Kratzer, and K. Jacobi, J. Appl. Phys. **95**, 7645 (2004).
- ¹¹D. J. Chadi, Phys. Rev. Lett. **59**, 1691 (1987).
- ¹²J. P. Perdew and A. Zunger, Phys. Rev. B **23**, 5048 (1981).
- ¹³D. M. Ceperley and B. J. Alder, Phys. Rev. Lett. **45**, 566 (1980).
- ¹⁴N. Troullier and J. L. Martins, Phys. Rev. B **43**, 1993 (1991).
- ¹⁵G. P. Srivastava, J. Phys.: Condens. Matter **5**, 4695 (1993).
- ¹⁶M. Bockstedte, A. Kley, J. Neugebauer, and M. Scheffler, Comput. Phys. Commun. **107**, 187 (1997).
- ¹⁷R. A. Evarestov and V. P. Smirnov, Phys. Status Solidi B **119**, 9 (1983).
- ¹⁸S. C. Erwin, A. A. Baski, and L. J. Whitman, Phys. Rev. Lett. **77**, 687 (1996).
- ¹⁹R. Miotto, G. P. Srivastava, and A. C. Ferraz, Phys. Rev. B **62**, 13623 (2000).
- ²⁰D. Paget, Y. Garreau, M. Sauvage, P. Chiaradia, R. Pinchaux, and W. G. Schmidt, Phys. Rev. B **64**, 161305(R) (2001).
- ²¹S. J. Jenkins and G. P. Srivastava, J. Phys.: Condens. Matter **8**, 6641 (1996).
- ²²R. Miotto, A. C. Ferraz, and G. P. Srivastava, Solid State Commun. **115**, 67 (2000).
- ²³J. Tersoff and D. R. Hamann, Phys. Rev. B **31**, 805 (1985).
- ²⁴R. Miotto, G. P. Srivastava, and A. C. Ferraz, Phys. Rev. B **62**, 13623 (2000).